94 GHz Three-Dimensional Imaging Radar Sensor for Autonomous Vehicles

Martin Lange and Jürgen Detlefsen, *Member, IEEE*

Abstract—**Sensing 3-D geometrical properties of an environment is essential for an autonomous vehicle operating in indoor situations such as production plants. Since the common acoustical and optical sensors fulfill this task insufficiently, this paper reports on an alternative approach using millimeter-wave images for real-time vehicle guidance. For application in the field of autonomous locomotion, the main advantage of this sensor concept is direct access to range and velocity information. System design and imaging results of a multitask 94 GHz pulse Doppler radar with 25 cm radial and 1.5° angular resolution are discussed. To point out specific millimeter-wave scattering phenomena, various radar images of typically structured indoor situations are presented. Extraction of information from sensor data, for example, obstacle detection, is demonstrated by radar image processing.**

I. Introduction

COMPARED with current approaches involving wire guidance, autonomous vehicles such as mobile robots promise substantially improved flexibility for use in future production plants. Autonomy in this case means that the vehicle is capable of sensing its surroundings and has sufficient intelligence to independently adapt its locomotion to an unknown and changing environment. Therefore, acquisition of relevant 3-D geometrical information through sensors is a key requirement in achieving genuine autonomy.

Different vehicle tasks, such as exploration of a structured but fully unknown scene, following a predetermined track, or docking at facilities, require various sensor operating modes combined with specific feature extraction from the measured data. The task of exploration usually requires a broad field of vision to generate radar maps and extract regions free of objects. For collision avoidance, object tracking, and vehicle reorientation during navigation, however, a more limited field of view is sufficient. The final task of interpretation of the obtained radar images, using artificial intelligence techniques leading to knowledge about the environment, is beyond the scope of this paper.

The common types of sensors providing suitable information for autonomous locomotion include standard video or stereo vision systems and acoustical proximity sensors with their restriction in maximum range. While video sensors offer excellent resolution at very high data rates, their ability to detect arbitrary objects under varying illuminations and calculate radial distance in real time is limited. Self-illuminating sensors with narrow beam widths using radar principles for range finding offer a promising solution to these limitations, keeping the necessary data processing power to a reasonable level [1], [2]. Laser scanners demonstrate good results, but as they must be used with an optical power low enough to avoid eye injuries, their detection range for arbitrarily shaped objects is typically limited to less than 10 m [3], [4]. Carrier frequencies in the millimeter-wave range allow coherent signal detection, resulting in a significantly increased sensitivity and instant access to range information [5]. The direct access to velocity information via Doppler processing is also an important feature when the sensor operates on board a maneuvering platform. As integrated subsystems for this millimeter-wave sensor are not yet available, the principal current drawback to industrial application is high cost.

To evaluate the relevance of sensor information for locomotion in structured indoor environments, a demonstrator vehicle equipped with various sensors has been built at the Technische Universität München. It carries on board a multitask millimeter-wave radar providing 3-D real-time information in a range from 0 to over 50 m, a close-range laser scanner, ultrasonic sensors, and wheel shaft encoders for incremental navigation. Current research activities concern the development of tailored routines for radar image analysis, task-related feature extraction, and the fusion of information received from different sensors.

II. Design Considerations and System Implementation

For internal representation, a segmentation of the actual indoor situation into volume cells—measuring approximately 20 cm in each dimension—is considered a reasonable compromise between the data flow to be processed in real time and the accuracy necessary for collision avoidance or vehicle guidance. Comparing different radar principles, the required high signal bandwidth of

Manuscript received August 7, 1990; revised December 10, 1990. This work was supported by the Deutsche Forschungsgemeinschaft (DFG), Sonderforschungsbereich 331.

The authors are with the Lehrstuhl für Mikrowellentechnik, Technische Universität München, Arcisstr. 21, D-8000 München, Germany.

IEEE Log Number 9143004.

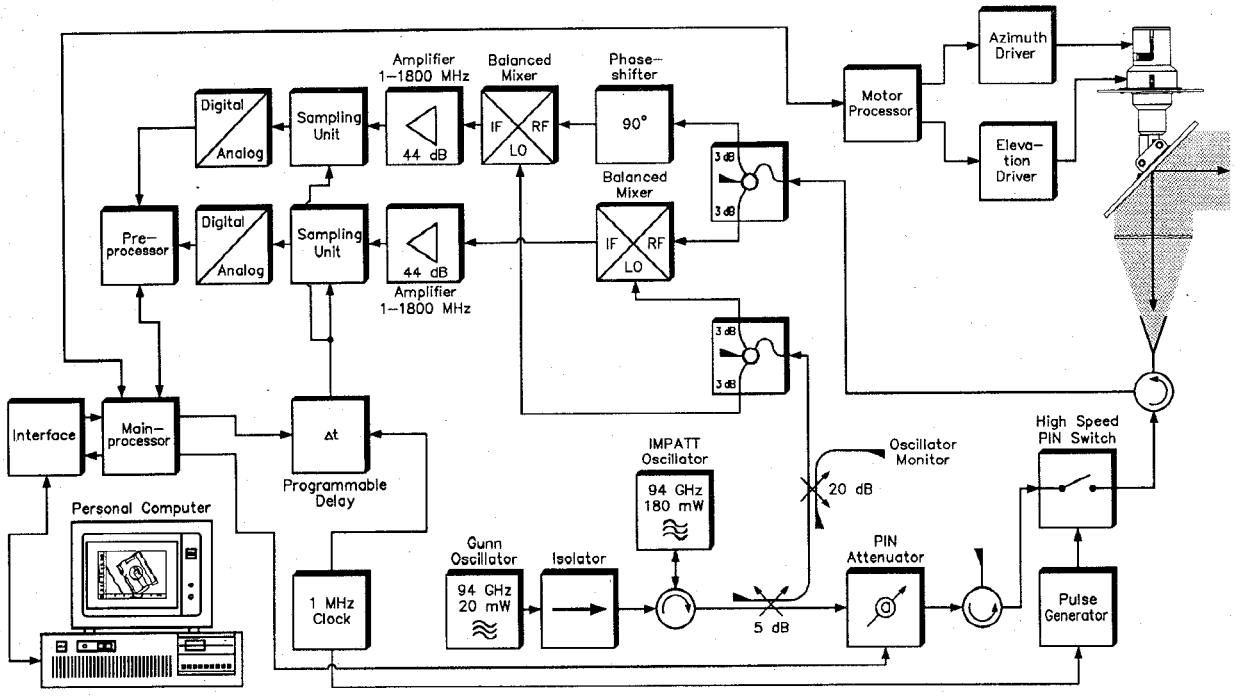

Fig. 1. Block diagram of a 94 GHz homodyne pulse Doppler 3-D imaging radar for an autonomous vehicle, operating in indoor environments.

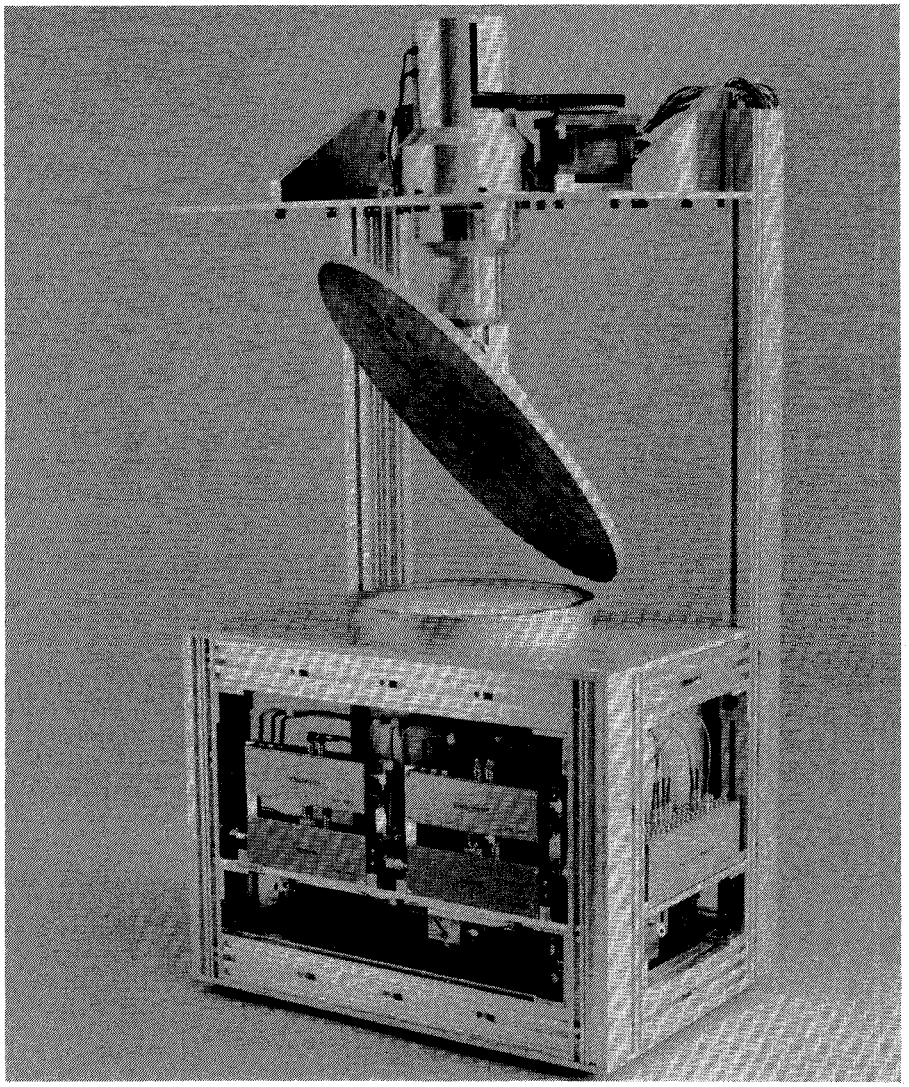

Fig. 2. View of sensor setup.

750 MHz can be obtained more easily by a single pulse or linear FM than by sophisticated coded pulse modulation techniques, which require very precise compression filters. The FM-CW principle was rejected because it requires a relatively time-consuming FFT to gain access to the range information. For maximum flexibility and full range gate control, a coherent single-pulse modulation scheme was finally chosen for this multitask sensor. The sacrifice in sensitivity resulting from not using a continuous wave system could be tolerated because of the near range application. Measurements demonstrated that sufficient object detectability is achieved when operating at distances typically up to 20 m. With an antenna diameter restricted to less than 20 cm, the required angular resolution can only be obtained at a high carrier frequency, e.g. 94 GHz. This also yields conveniently high Doppler frequencies of 625 Hz per 1 m/s, which permit accurate velocity measurements within a short observation time.

Transmitter power is generated by a stable Gunn oscillator which injection locks a 180 mW CW IMPATT source, as shown in Fig. 1. This is followed by an ultrafast p-i-n switch for coherent pulse modulation [6], [7]. This passive modulation scheme guarantees nearly perfect coherence across the 1.7 ns pulse width, which is necessary for Doppler processing at 94 GHz carrier frequency, but adds nearly 5 dB loss to the transmitter path. Active pulse generation by pulsing a solid-state source would significantly increase output power but requires a very careful design to maintain stable coherence across the subnanosecond rise and fall times. The CW power incident to the p-i-n pulse modulator can be decreased by a maximum attenuation of 30 dB to shift the sensor's dynamic range to accommodate strong specular reflections. For a maximum unambiguous range of 150 m, pulses can be transmitted at a repetition frequency as high as 1 MHz. The losses of all components within the transmitter path add up to 13 dB, leading to a transmitted pulse peak power of 10 mW. Although the efficiency of this scheme is rather low, the benefits are very high resolution and coherence of the transmitted signal.

As shown in Figs. 2 and 3, a fixed radar front end in combination with a scanning reflector was chosen to maintain low inertia. The far-field beam width of 1.5° in azimuth and elevation is generated by a lens of 168 mm diameter, illuminated by a corrugated horn for polarization decoupling. Because of the high antenna gain, scatterers within a range of approximately 10 m are observed under near-field conditions. In this range the angular resolution and radar sensitivity are apparently decreased. A calculation of the antenna's near-field power distribution, displayed in Fig. 4, indicates a fairly parallel beam of 20 cm diameter until far-field conditions are reached, where the beam starts widening to 1.5°. The reflector was designed to permit fast scanning modes as well as focused looks at objects of interest via servo motors. Scattering data from up to 10^4 volume resolution cells—measured at three full azimuth turns or three looks to arbitrary directions—can be measured per second.

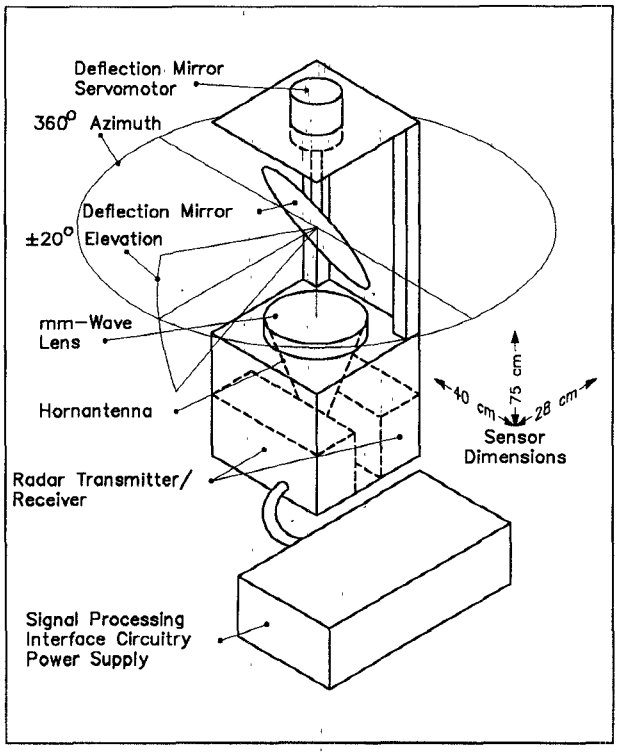

Fig. 3. Field of vision of 94 GHz 3-D imaging sensor.

The sensor down-converts the received signals directly to baseband via a homodyne quadrature mixer. This is different from usual heterodyne radar designs and has the advantage of reducing the number of components. Since baseband frequencies start at a high PRF (1 MHz), no substantial $1/f$ noise contributions appear. This results in a receiver noise figure of 12 dB, which is comparable to a heterodyne approach.

Leakage of the p-i-n switch between transmitted pulses in this design has no effect on the receiver, since the resulting dc signal is fully suppressed by the baseband amplifiers. In this setup a p-i-n switch on/off ratio of 20 dB modulates nearly all available carrier power without limiting the receiver's dynamic range. Although not necessary in practical use, information loss caused by suppression of the return signal's dc component could be recovered by referring all signals to the average signal level measured at distant regions where, obviously, no return signal is received. At short signal delays of less than 1 μs, equivalent to 150 m distance, the coherence length of even a free-running Gunn oscillator turns out to be high enough to allow precise Doppler measurements [8], [9].

I and Q components of baseband pulse trains are broad-band amplified, sampled, and converted to a digital format. The range gate position is defined by a programmable delay between pulse and sampling trigger. For precision measurements, requiring oversampling of the received pulses, the range gate can be positioned by increments of 2.8 cm, corresponding to 186 ps delay increments. Since each pulse train is sampled once, information can be obtained from only a single range gate at

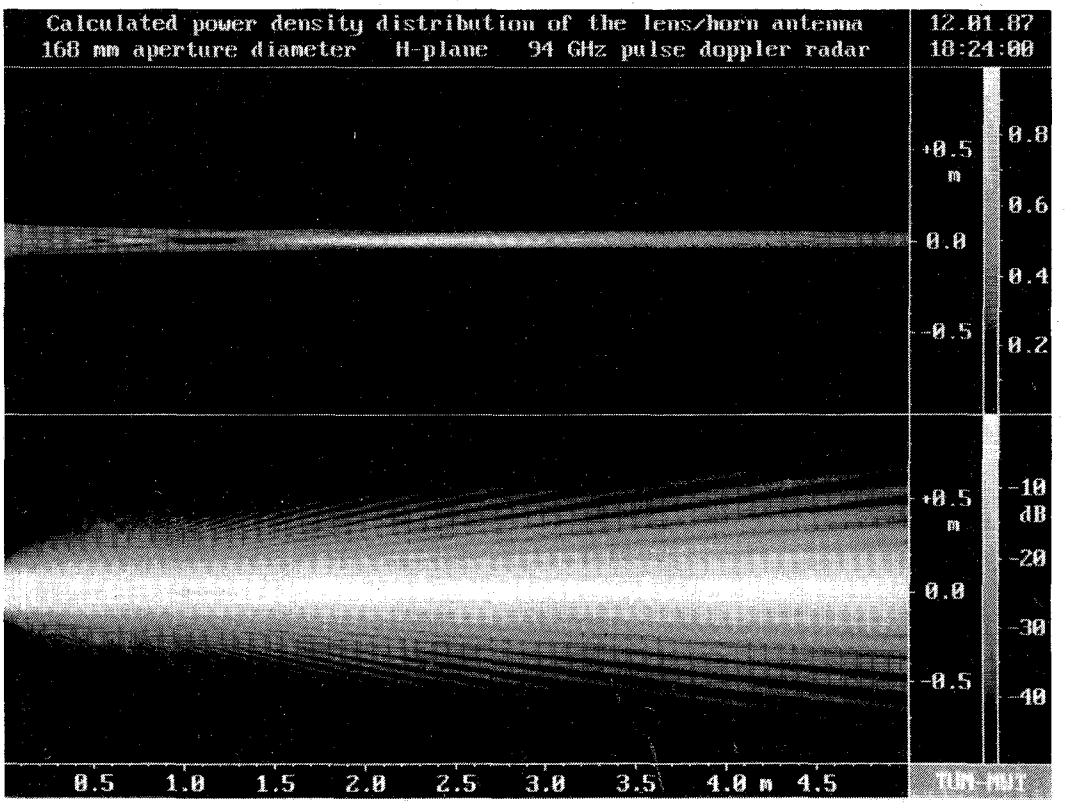

Fig. 4. Calculated power distribution within the antenna near field, displayed in linear scale (upper figure) and logarithmic scale (lower figure).

TABLE I
SYSTEM PARAMETERS

Operating frequency	94.0 GHz
Wavelength	3.19 mm
Oscillator power	180 mW
Transmitted pulse peak power	10 mW
Pulse repetition frequency	1 MHz
Unambiguous range	150 m
Pulse width	1.7 ns
Effective signal bandwidth	±290 MHz
Resolution	25 cm
Smallest range gate displacement	2.805 cm
Unambiguous speed	±8.0 m/s
3 dB antenna beam width	1.5°
Data rate	10^4 volume cells/s

one time. In this case, scanning in range is done by sequentially shifting the range gate across the region of interest. Current activities aim to eliminate this bottleneck by replacing the samplers with high-speed A/D converters, capable of handling bandwidths up to 500 MHz. Problems then arise in reducing the data flow of several Gb/s down to typically 200 kb/s by numerical averaging within each individual range gate. In the single sampler design, illustrated in Fig. 1, an analog low-pass filter following the sampler integrates over 100 pulse periods, resulting in a maximum information rate of 10^4 volume cells per second with 12 b signal resolution.

Three processors are in charge of radar signal processing as well as the timing and data management of the system itself, so that low-level functions such as Doppler analysis and beam control can be performed simultaneously with high-level functions such as recognition of paths free of obstacles, generation of radar maps, or navigation. Working in parallel, about 5000 measurements per second can be processed when high-level functions are performed. For guidance of a platform maneuvering with velocities up to 0.1 m/s this figure turned out to be sufficient.

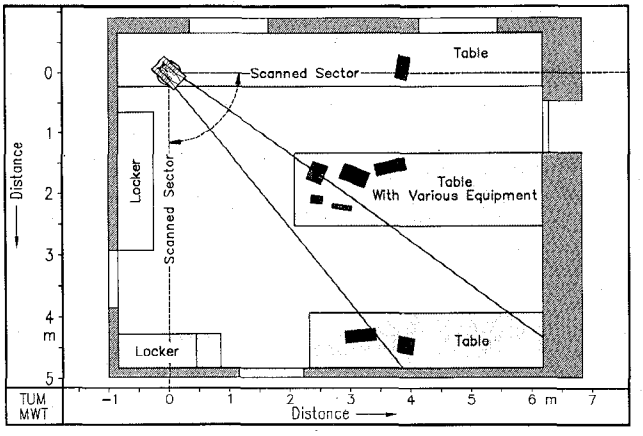

Fig. 5. Top view schematic of laboratory scene for the preliminary radar imaging experiments at 35 GHz, with the sensor location indicated near the upper left corner.

III. IMAGING PERFORMANCE AT 35 GHz AND 94 GHz

Because of the requirement for real-time data acquisition, the millimeter-wave image is generated by interpret-

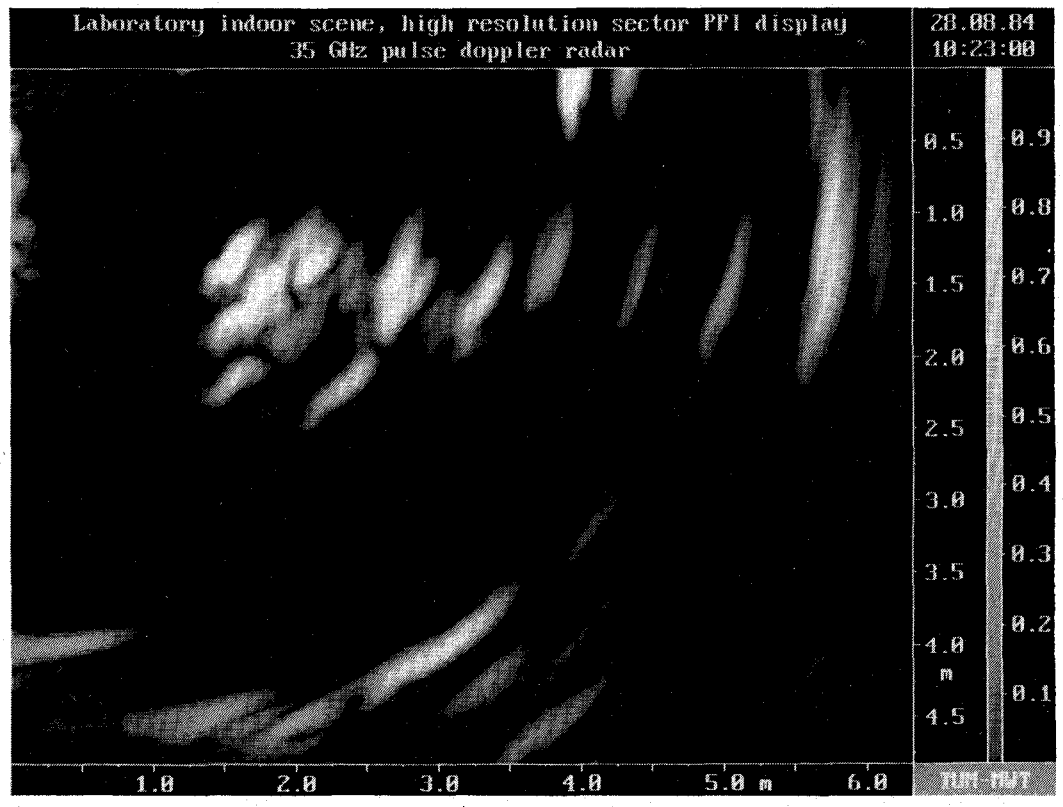

Fig. 6. 35 GHz 2-D radar image of scanned 90° sector in Fig. 5. Measurements were taken on a polar grid with 0.82° and 4.2 cm increments.

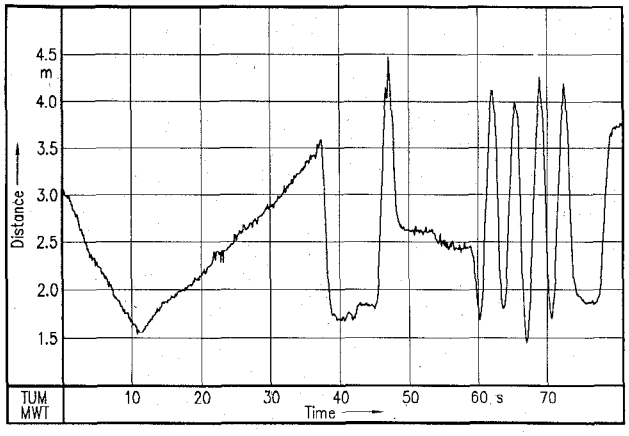

Fig. 7. Radially tracked location of a person moving arbitrarily within the sensor's main lobe.

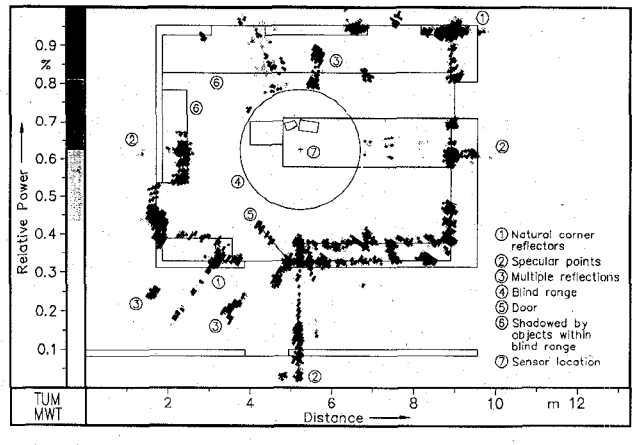

Fig. 8. 2-D horizontal distribution of backscattered power at 94 GHz. For better orientation, the actual laboratory contours are outlined.

ing the received signal as a measure of the density of point scatterers within an observed volume cell. Based on this linear scattering model, where interactions between individual point scatterers are not taken into account, such effects as interference, multiple reflections, shadowing, or absorption require a considerable amount of interpretation to derive the actual geometry from the measured millimeter-wave radar image.

Prior to the development of the mentioned 94 GHz sensor, basic experiments at 35 GHz were carried out to evaluate preliminarily the quality of radar images of indoor environments. Since both systems are operated with antenna apertures of equal size, the 35 GHz pulse Doppler sensor showed practically the same system parameters as those listed in Table I except with a 4° beam width. The first test scene was a laboratory, as outlined in Fig. 5. The sensor was located on a table, and scanned horizontally a 90° sector where numerous objects were arranged. The corresponding 35 GHz radar image, in Fig. 6, shows several reflections with angular broadening, caused by the 4° antenna beam pattern. While objects with rough surfaces, showing diffuse scattering, would consist of many point scatterers, representing the actual geometry, most received signals seem to refer more to specular reflec-

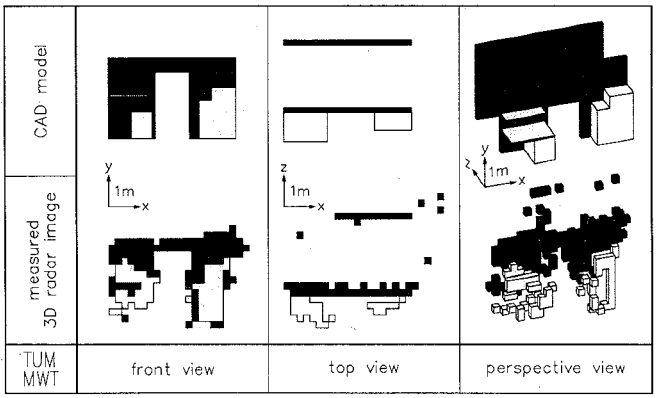

Fig. 9. Reconstructed 3-D geometry of an indoor scene (walls, door, table, locker) based on $20 \times 20 \times 20$ cm^3 volume cells in comparison with the actual geometry.

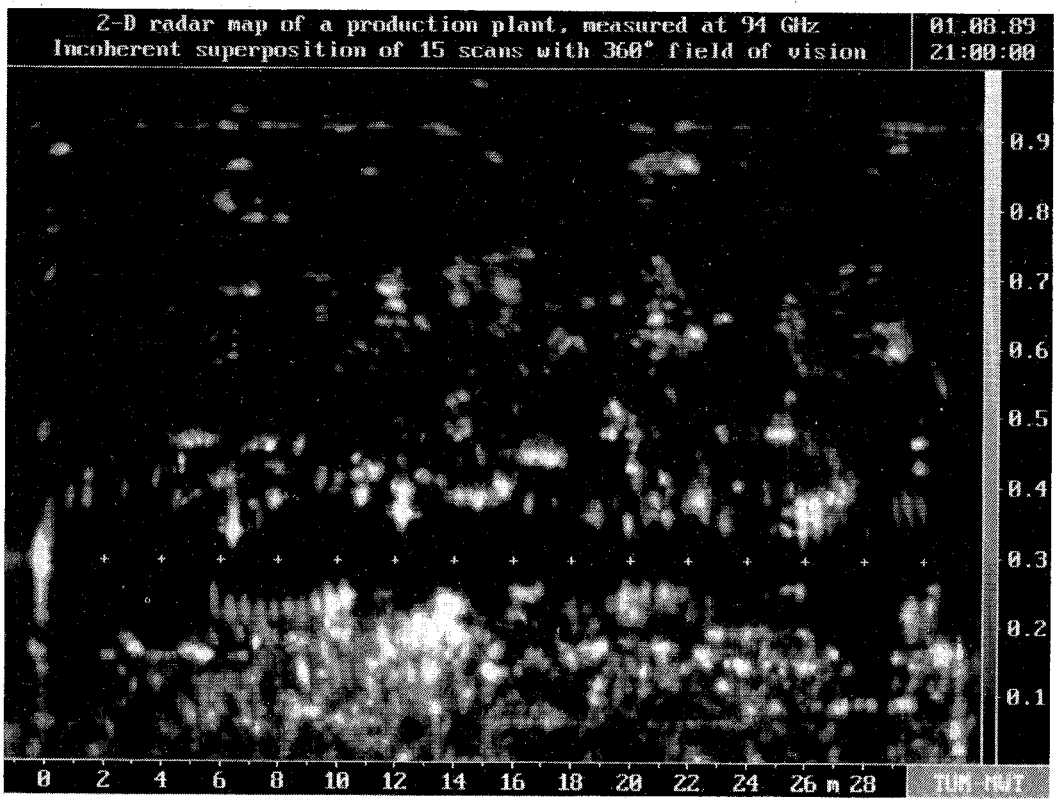

Fig. 10. 2-D radar map of a production plant generated from 15 scans along a straight path.

tions, giving no indication of the outlines and boundaries. In the left half of the radar image, areas free of obstacles appear mainly undisturbed, while artifacts seem to cover these areas when objects are in front.

Besides the evaluation of the complete radar image, the ability to detect and track moving objects within these scenes was also examined. Direct motion measurement via Doppler processing gives millimeter-wave sensors the unique ability for precise range tracking. The stability of an early- and late-gate range tracking loop can be improved when the prediction of the object distance within one measurement interval is supported by accurate Doppler velocity information. For radial tracking, the exact object location and velocity are calculated from scans of about 50 cm length, which are centered at the estimated object distance. Within the tracking loop, estimates for the new object location are determined by linear prediction, performed every 20–80 ms, depending on the number of simultaneously tracked objects. To demonstrate this ability under realistic conditions, a person moving randomly to and fro was tracked radially, as shown in Fig. 7. Random reflectivity fluctuations exceeding even 20 dB, caused by quickly varying interferences, are handled by cell averaging constant false alarm rate (CFAR) algorithms. By calculating the return signal to noise ratio for each range gate within a scan, CFAR

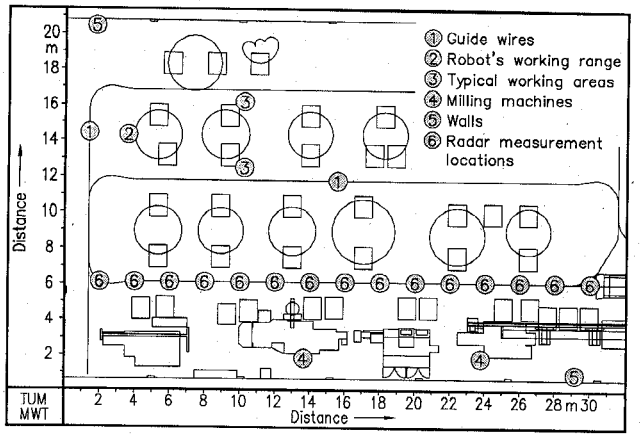

Fig. 11. Top view schematic of the imaged production plant with outlines of machines and the robot's work areas.

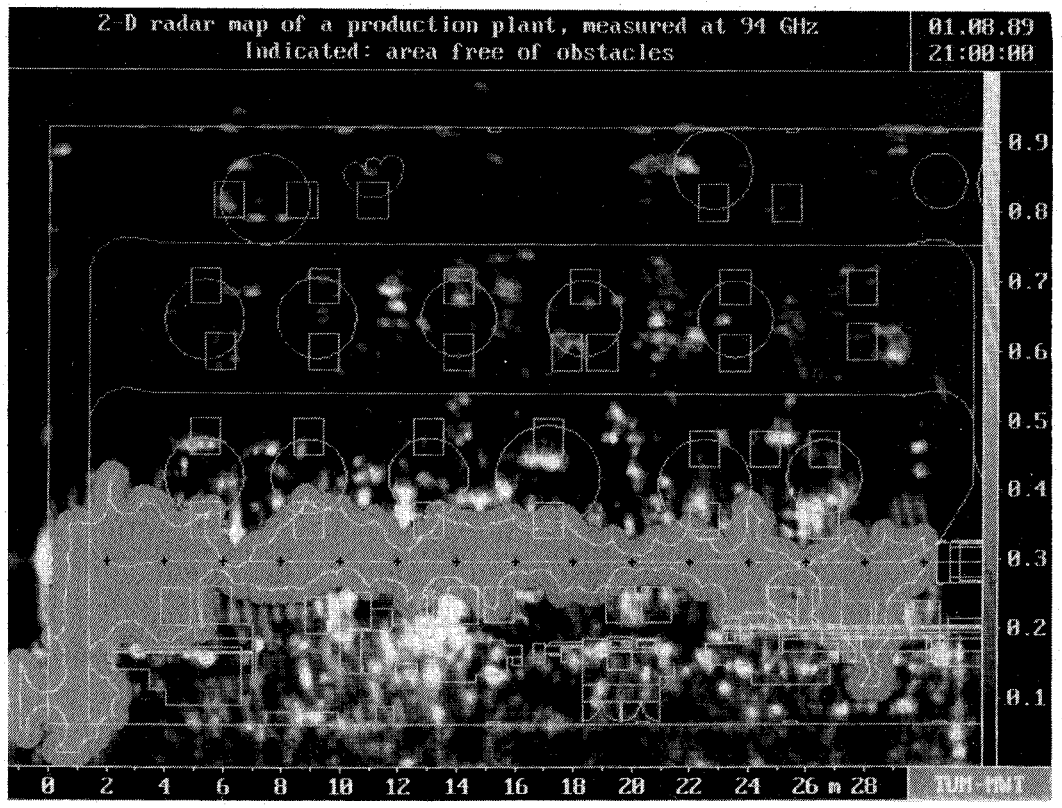

Fig. 12. Area free of obstacles along the scanned path, extracted by radar image processing.

algorithms accomplish a reliable object detection with a reasonable numerical effort. Verification measurements at 35 GHz performed on a pendulum serving as a well-defined moving scatterer proved to be accurate within 3 cm. Angular tracking by dithering the main lobe with the deflection mirror turned out to be too slow for close ranges where significant glint and high angular accelerations occur. A conical scanning device, implemented at the antenna feed, will overcome this limitation, significantly reducing the time for pointing error measurements.

Encouraged by preliminary results obtained at 35 GHz, the following imaging experiments were carried out with the aforementioned 94 GHz sensor to obtain better angular resolution and higher diffuse backscattering from rough surfaces. The laboratory scene viewed in Fig. 5 was scanned again, this time with the sensor located in the middle of the room, covering 360° in azimuth. As expected, the obtained 94 GHz radar image in Fig. 8 shows a satisfying resolution and gives a better representation of the actual contours than did the 35 GHz image. Full recovery of the receiver from saturation during monostatic pulse transmission takes 9 ns, causing a decreased sensitivity within a range of 1.4 m radius. Although some diffuse scattering can be observed, specular reflections still appear to be dominant, sometimes exceeding the receiver's dynamic range of nearly 70 dB. These spots

appear either on flat surfaces or, frequently, on dihedral or trihedral configurations where the transmitted beam is directly reflected to the antenna. Fortunately, artifacts caused by multiple reflections or receiver saturation always appear at greater distances. Therefore, obstacle detection algorithms, usually applied only up to the nearest reflection, are not affected. Consequently, radar maps based on these images should be assembled from only the nearest reflection detected.

To provide an example of the sensor's 3-D imaging abilities, the lower left sector of the laboratory scene, displayed in Fig. 5, was scanned from a single location in range, azimuth, and elevation. For this measurement angular increments of 1° and radial increments of 5.6 cm were chosen. For verification of the objects extracted from 94 GHz scattering measurements, Fig. 9 displays a simplified CAD model of the structured scene, composed of walls, furniture, and a doorway. Object extraction is realized first by transforming the polar data to a rectangular coordinate system aligned parallel with the actual geometry. Then a 3-D CFAR scheme is used to mark those volume cells in which the backscattered power exceeds the receiver noise level by, typically, 7 dB. All marked volume cells, each measuring 20 cm in each dimension, are displayed in Fig. 9. For better visualization, gray scales are assigned manually to different layers on the z axis. Although the detail of object reconstruction suffers and several volume cells are missing because of a lack of backscattered signals, the basic topology of the scene appears. A more solid representation of the scene can be achieved when images are superimposed that are measured from different aspects.

The next step toward vehicle guidance by millimeter-wave radar sensors is to take multiple looks of a stationary scene from different locations. A realistic environment for these trials was a production plant with various machines and with stationary robots with lanes for wire-guided transportation vehicles between them (Fig. 10). The plant was scanned horizontally along a straight path from 15 locations, spaced by 2 m, as marked in Fig. 11. In this case, reference coordinates defining the exact sensor location were provided externally, but they can in principle also be derived from the images. By incoherently superimposing all 15 full scans in Fig. 10, a 2-D radar map can be generated for navigation and route planning. For collision avoidance, paths free of obstacles can be determined by converting the analog radar image by a 2-D CFAR detector to a binary radar image and convolving it by the outline of the vehicle. Adjacent pixels then form an area free of obstacles, as demonstrated in Fig. 12, where a cylindrical vehicle geometry is assumed. The inner boundary line defines the maximum position to which the vehicle's center may be moved.

Radar data measured only from the current location would be available for detection of obstacles ahead during exploration of unknown environments. Taking this into account, the original noncausal obstacle detection scheme was modified by refining measurements taken from areas ahead while passing by. Simulated explorations along the measured lane lead to satisfying results, comparable to those in Fig. 12.

IV. Conclusion

The results discussed demonstrate that for guidance of autonomous vehicles, the extraction of geometrical properties of the environment in real time is a promising approach, especially in ranges exceeding a few meters, where most other sensors fail. Although millimeter-wave frequencies at 94 GHz and very high modulation bandwidths are necessary for precise close-range radar images, causing sensitivity trade-offs, signal quality seems to be sufficient for the given task. The authors believe that by integrating the current discrete waveguide assembly into an advanced, compact module, the transmitted pulse peak power could be increased by as much as 4 dB. While 2-D scanning can be performed close to real time with a data flow of up to 10^4 volume cells per second, three dimensions cannot be scanned and processed fast enough for vehicle control at the present time. Measurement and processing efficiency might be increased by focusing on regions of interest, requiring suitable strategies and information in advance.

References

[1] J. Detlefsen, M. Lange, and M. Bockmair, "Evaluation of near range 94 GHz radar images for autonomous vehicles," in *Proc. Int. Conf. Radar* (Paris), Apr. 1989, pp. 203–208.

[2] M. Lange and J. Detlefsen, "94 GHz 3D-imaging radar for sensor-based locomotion," in *IEEE MTT-S Int. Microwave Symp. Dig.* (Long Beach), June 1989, pp. 1091–1094.

[3] Ch. Fröhlich, G. Karl, and G. Schmidt, "Sensor assisted navigation of a mobile robot in building environments," presented at IEEE Int. Workshop on Sensorial Integration for Industrial Robots Architectures + Applications (Zaragoza), Nov. 1989.

[4] G. Karl, F. Freyberger, and G. Schmidt, "Data processing for a 3-D range imaging laser camera applied to real-time operations of a mobile robot," in *Proc. 2nd Int. Workshop on Manipulators, Sensors and Steps Towards Mobility* (Manchester), 1988, pp. 18.1–18.18.

[5] J.-Ch. Bolomey, "Recent European developments in active microwave imaging for industrial, scientific, and medical applications," *IEEE Trans. Microwave Theory Tech.*, vol. 37, pp. 2109–2117, 1989.

[6] M. Lange and J. Detlefsen, "A 35 GHz homodyne pulse-Doppler radar with very high resolution for short range application," in *Proc. Int. Conf. Radar* (Paris), May 1984, pp. 210–214.

[7] M. Lange, J. Detlefsen and M. Bockmair, "Resonant pulse amplification for radar imaging applications," in *Proc. 15th European Microwave Conf.* (Paris), Sept. 1985, pp. 1005–1009.

[8] F. Nathanson, *Radar Design Principles*. New York: McGraw-Hill, 1969, p. 340.

[9] M. Skolnik, *Radar Handbook*. New York: McGraw-Hill, 1970, ch. 17–49.

Martin Lange was born in Munich, Germany, on September 10, 1958. He received the Dipl.-Ing. degree from the Technische Universität München in 1983, and he joined the Microwave Institute there in 1984. Currently he is pursuing the Ph.D. degree as a research assistant. His areas of interest include close-range radar sensors with high resolution at millimeter-wave frequencies for industrial applications.

Jürgen Detlefsen (M'82) received the Dipl.-Ing. (M.Sc.) degree in 1967, the Dr.-Ing. (Ph.D.) degree in 1971, and the Habilitation degree in 1978 from the Technische Universität München, Germany.

From 1967 to 1980 he worked in the field of millimeter-wave techniques; his main interests were microwave generation by semiconductors, impedance measuring techniques, near-field radar systems, and microwave imaging methods. In 1980 he received the Award of the German ITG Society. Since 1980 he has been Professor of Radar Systems and Radio Navigation Systems at the Technische Universität München, where in 1988 he was appointed for the field of electromagnetic fields and circuits. In 1987 he obtained a fellowship from the Japan Society for the Promotion of Science. His current research interests are primarily concerned with inverse scattering and microwave optics, with special emphasis on industrial applications of microwave imaging, such as the field of robotics.

Dr. Detlefsen is a member of URSI Commission B and of ITG.